LANGMUIR

pubs.acs.org/Langmuir Article

Thermodynamics and Kinetics of a Binary Mechanical System: Mechanisms of Muscle Contraction

Josh E. Baker*

Cite This: *Langmuir* 2022, 38, 15905−15916 Read Online

ACCESS | Metrics & More | Article Recommendations

ABSTRACT: Biological motors function at the interface of biology, physics, and chemistry, and it remains unsettled what rules from which disciplines account for how these motors work. Myosin motors are enzymes that catalyze the hydrolysis of ATP through a mechanism involving a switch-like myosin structural change (a lever arm rotation) induced by actin binding that generates a small displacement of an actin filament. In muscle, individual myosin motors are widely assumed to function as molecular machines having mechanical properties that resemble those of muscle. In a fundamental departure from this perspective, here, I show that muscle more closely resembles a heat engine with mechanical properties that emerge from the thermodynamics of a myosin motor ensemble. The transformative impact of thermodynamics on our understanding of how a heat engine works guides a parallel transformation in our understanding of how muscle works. I consider the simplest possible model of force generation: a binary mechanical system. I develop the mechanics, energetics, and kinetics of this system and show that a single binding reaction generates force when muscle is held at a fixed length and performs work when muscle is allowed to shorten. This creates a network of thermodynamic binding pathways that resembles many of the characteristic mechanical and energetic behaviors of muscle including the muscle force−velocity relationship, heat output by shortening muscle, four phases of a muscle tension transient, spontaneous oscillatory contractions, and force redevelopment. Analogous to the thermodynamic (Carnot) cycle for a heat engine, isothermal and adiabatic binding and detachment reactions create a thermodynamic cycle for muscle that resembles cardiac pressure−volume loops (i.e., how the heart works). This paper provides an outline for how to re-interpret muscle mechanic data using thermodynamics − an ongoing effort that will continue providing novel insights into how muscle and molecular motors work.

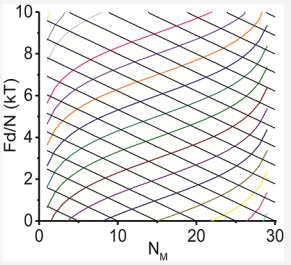

INTRODUCTION

Many biomechanical mechanisms involve metastable protein structural switches that both affect and are affected by a mechanical potential. For example, a conformational change in a protein (M) induced by ligand (A) binding can generate a mechanical potential (e.g., generate force in a compliant element) upon binding (M to AM in Figure 1A). Inversely, a mechanical potential can reverse that conformational change, inducing the dissociation of the ligand (AM to M). A collection of protein switches that reversibly generate force in thermally equilibrated compliant elements constitutes a binary mechanical model system. Binary model systems are often used to illustrate basic principles of statistical mechanics with the typical example being that of a binary magnetic model system consisting of spins in a magnetic field;[1] however, a binary mechanical model system applicable to an ensemble of protein switches remains undeveloped. Having previously solved the steady state case using a mean force field approach;[2] here, with the formal construction of a system spring that defines the mechanical potential, I solve the more general case of force generation. In a series of publications, I develop the model and its implications for muscle contraction, showing that it reconciles disparate models of molecular motor mechanochemistry[3] and accurately accounts for steady-state[2] and transient muscle mechanics and energetics.

A muscle fiber, or cell, contains large protein assemblies arranged around interdigitated filamentous arrays of actin and myosin molecules within which an individual myosin cross-bridge (or motor) generates force upon strongly binding to an actin filament.[4,5] The basic mechanism is well established. The formation of a strong bond with actin induces a bend in the myosin motor (a lever arm rotation) that displaces an actin filament a distance d of ∼8 nm (Figure 1A).[6−12] Single molecule studies show that these events occur within a millisecond of each other as a single mechanochemical step.[5,13,14] The stiffness, κ_{trap}, of an optical spring displaced in these experiments can be set to values ranging from 0.1 to 1.0 pN/nm, resulting in motor-generated forces, $\kappa_{trap} \cdot d$, ranging from 1 to 10 pN, and mechanical potentials, $1/2\kappa_{trap} \cdot d^2$,

Received: June 20, 2022
Revised: November 17, 2022
Published: December 15, 2022

https://doi.org/10.1021/acs.langmuir.2c01622
Langmuir 2022, 38, 15905−15916

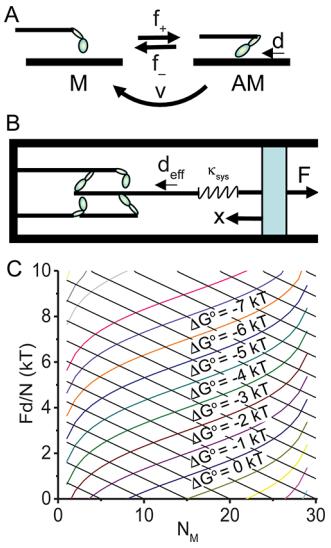

Figure 1. Binary mechanical model system. (A) Two-state (M and AM) scheme in which a single motor (blue ovals) undergoes a discrete conformational change upon binding to a track (black rectangle), generating a displacement, d, at a rate f_+ (M to AM). The reverse transition occurs at a rate f_- (AM to M). Motors can be irreversibly detached (AM to M) through an active (ATP-dependent) process that occurs at a rate v. (B) If a single system spring with stiffness κ_{sys} equilibrates with the surroundings, F determines the distribution of states between M and AM (eq 4). If force generation either occurs against a fixed length (no movement, x, of the blue bar) or occurs much more rapidly than the spring equilibrates with the surroundings, F is mechanistically determined by working steps (eq 3) that displace the system spring an effective distance, $d_{eff} = d/(a{\cdot}N)$. (C) Equation 4 (colored curves) is plotted at ΔG° increments of 1 kT, and eq 3 is plotted (black lines) at N_M° increments of 5.

ranging from 3 to 30 pN·nm. This force-generating step, referred to as the working step, is an intermediate step (M to AM, Figure 1A) in the motor-catalyzed hydrolysis of ATP to products ADP and P_i.[15−17] In myosin motors, the working step occurs upon release of P_i. A net flux through the working step is generated through the ATPase reaction when myosin motors are irreversibly transferred from AM to M following ADP release and ATP binding and hydrolysis (v in Figure 1A). We have shown that in in vitro assays, the myosin working step is reversible[18] with rate constants (f_+ and f_- in Figure 1A) that depend on an external mechanical potential.[19] In short, myosin is a metastable protein switch that both generates and responds to an external force. The question remains, what is the relationship between the mechanochemistry of this protein switch and the mechanochemistry of muscle?

In the early 1900s, A.V. Hill made precise measurements of work, w, and heat, q, output by shortening muscle, establishing the experimental foundation for a thermodynamic description of muscle contraction, which he first published in 1938.[20,21] According to Hill, when muscle shortens a distance, x, against a constant force, F, the chemical energy available for work by shortening muscle $\Delta G(F)$ is transferred at a rate, v, to the surroundings as work, $w = F{\cdot}x$, and heat, q, or

$$v{\cdot}\Delta G(F) = F{\cdot}V + dq/dt$$

Here, V (= dx/dt) is the rate of muscle shortening (i.e., velocity) and dq/dt is the rate of heat output by shortening muscle. This is classic chemical thermodynamics where chemical energy and free energy transfer are defined at the level of the muscle system, consistent with experimental studies.[18,19,22−24]

In 1938, little was known about the chemistry underlying $v{\cdot}\Delta G(F)$ and dq/dt, yet Hill was convinced that these terms had a molecular basis. He wrote, "measurements of heat production are no substitute for direct chemical analysis. But they do suggest problems to the chemist and provide a framework into which his detailed machinery must be fitted".[25] However, in the 1950s, static electron micrographs of muscle revealed individual myosin crossbridges protruding from myosin filaments and interacting with adjacent actin filaments with each crossbridge (motor) positioned to function as an "independent force generator".[26,27] Dreams of muscle as a crystalline lattice containing mechanically isolated motors inspired a bottom-up mechanical determinism incongruent with chemical thermodynamics.[28] In 1957, A.F. Huxley proposed a molecular mechanic framework for muscle contraction (the power stroke model) that was formalized by T.L. Hill in 1974[29] and has since been the foundation for most models of molecular motors and muscle to date.

The difference between A.V. Hill's thermodynamic model and the Huxley−Hill model is profound and historical. T.L. Hill was compelled to develop a new theoretical framework because the basic assumption in Huxley's model − that the force of muscle is determined from the springs of myosin molecules − is inconsistent with thermodynamics. This assumption, however, aligns with Robert Boyle's 17th century corpuscular mechanical philosophy[30] that the force of a system is determined from the springs of molecules in that system. Relating the volume of air in a container to the space occupied by the coiled springs of air molecules, Boyle described his observation that the volume of air decreases inversely with increased pressure (Boyle's law) as the springs of air being compressed by the surrounding force.[30] He referred to these experiments as "touching the springs of air".

In 1699, based on his observation that the pressure of a gas increases linearly with temperature, Guillaume Amontons designed the first hot air engine, demonstrating that mechanical work can be performed through the cyclic heating and cooling of air.[31] Amontons then described the first mechanism for a heat engine using Boyle's corpuscular mechanic philosophy. Amontons reasoned that the substance of heat tensions the coiled springs of air to generate pressure, and the subsequent expansion of the springs into a new volume performs work. This is precisely Huxley's power stroke mechanism applied to air molecules. Analogous to Amontons' model, Huxley proposed that the chemical energy for ATP hydrolysis somehow tensions a myosin spring to generate force after which the spring shortens with muscle to perform work (a molecular power stroke). Thermodynamics transformed our understanding of heat engines,[32] but the thermodynamic revolution has yet to reach many areas of molecular biology. Notwithstanding appeals from A.V. Hill,[20,25] my students, and myself,[2,3,23] thermodynamics has had little impact on our current understanding of the mechanism of muscle contraction.

In the 18th and 19th centuries, kinetic theory and thermodynamics showed us that thermodynamic forces are contained within the walls that constrain them (within system springs) not within molecules that somehow hold their own force (within molecular springs), demonstrating that corpuscular mechanics attributes to molecules the mechanical properties of the system that contains them. While molecules

https://doi.org/10.1021/acs.langmuir.2c01622
Langmuir 2022, 38, 15905−15916

can and do generate force through collisions and binding, the magnitude of the force generated by a system of molecules is determined by system energetics: temperature for a gas and binding free energy for motors, neither of which is defined or determined from within a molecule (binding free energy is defined by a non-equilibrium concentration gradient of motors between the M and AM states). The free energy for ATP hydrolysis perturbs a muscle system from equilibrium by irreversibly transferring myosin motors from AM to M through a catalyzed reaction. Thus, the free energy for ATP hydrolysis is used to increase the binding free energy (not tension a corpuscular spring), and work is performed when the binding reaction equilibrates (not when a corpuscular spring shortens).

Nevertheless, Boyle's corpuscularian philosophy remains popular in molecular biology where proteins are often depicted as corpuscles that embody the properties of the physiological system within which they function.[33] Boyle's "springs of air" and Huxley–Hill's springs of myosin illustrate how molecular mechanisms inferred through this approach are grossly inventive. Over the past 50 years, in response to new experimental results, Huxley–Hill models of muscle contraction have consistently expanded to include more states,[34] more molecular springs (both linear and non-linear),[35] more spatial explicitness,[36] additional kinetic transitions (each with their own arbitrary strain-dependent rates),[37] and new mechanical elements.[38,39] These mechanisms are Rube Goldberg-esque in that they describe a simple two-state system using tiny versions of structural scaffolding and mechanical components manufactured as needed to formally define, constrain, and control molecular forces for the sole purpose of making molecular forces "determine" the macroscopic force. There is no limit to one's imagination when building these machines. Consider, for example, Boyle's description of an air molecule as a "piece of ribband, that is, to be very long, slender, thin, and flexible lamina, coiled or wound up together as a cable, piece of ribband, spring of a watch, hoop, or the like."[30] Gibbs described such efforts at building reasoned corpuscular machinery as "rational mechanics", which he dismissed as seeking "mechanical definitions of temperature and entropy."[40]

Gibbs describes thermodynamics as "the laws of mechanics for such systems [of particles] as they appear to beings who have not the fineness of perception to enable them to appreciate quantities of the order of magnitude of those which relate to single particles."[40] In other words, our best attempts at rational mechanisms will always be too large, too few, and non-physical. Thus, springs in biological systems cannot be defined as rational mechanical devices; they can only be defined as thermodynamic constructs that describe the change in energy of a system of particles when that system of particles is stretched (or compressed).

A single protein is a system that contains many (sometimes thousands of) atoms. Because we are incapable of easily comprehending the energetic changes associated with the distortion of every atomic bond that occurs within a protein when stretched, a protein spring is defined as a thermodynamic construct to approximate the protein energy-extension relationship. Indeed, when we mechanically constrain the length of a protein, the "laws of mechanics" of that protein as they appear to us can be approximated with a molecular spring.[41] However within a muscle cell, millions of proteins are contained within thermally fluctuating macromolecular assemblies, and molecular springs are no longer valid thermodynamic constructs. Nevertheless, Huxley–Hill defines molecular springs in muscle by assuming that infinitely rigid local structural constraints insulate these rational molecular springs from their surroundings. We have shown that no such structural constraints exist,[19,22,23,42] which is to say that rational molecular springs cannot be defined. The length and force of the muscle system, however, can be constrained, in which case the "laws of mechanics" of muscle as they appear to us can be approximated by a single muscle spring.

A thermodynamic muscle spring describes the laws of mechanics of a muscle fiber, and from the mechanical state of that spring, chemical thermodynamics provides a framework for determining the biochemistry (the most probable distribution of states) of the molecules contained within that system. The formal difference then between rational mechanic (Huxley–Hill) and chemical thermodynamic models of muscle is clear and significant. According to Huxley–Hill, the biochemistry and mechanics of a given myosin motor in muscle are defined at the level of the motor independent of muscle force, and muscle force is formally determined from individual motor forces. In a chemical thermodynamic model, the biochemistry and mechanics of a motor ensemble are determined from muscle force. Philosophical debates aside, formal arguments over which model describes the "laws of mechanics of such a system" were settled centuries ago.

What remains then is to formally construct a system spring that accurately describes the "laws of mechanics" of an ensemble of molecular switches. These laws differ from those of a single motor spring in two ways. First, a molecular spring describes the force generated by a single motor, which is dissipated when that motor is detached (M), whereas a system spring describes a system force that is cumulatively generated by all motors in the system and is maintained even when all but one of those motor is detached. Second, this system spring contains molecular switches (motors in the M or AM state), and the force of the spring determines the probability distribution of these switches between the M and AM states. Like other elastic systems containing mechanical switches [e.g., titin[41] and rubber[43]], here, I show that the mechanics of this system can be described by an entropic spring. With a system spring thus constructed, I establish the kinetics and thermodynamics of a binary mechanical system.

Adiabatic force generation and isothermal work are described by two separate equations. When the system is held at a fixed length, the binding reaction collectively generates force in the system spring. When the system is allowed to shorten, work is performed along the binding isotherm. Depending on the external system constraints (fixed length versus isothermal), a single binding step can occur through either of these processes, creating a network of thermodynamic binding pathways. I show here that different pathways resemble different characteristic mechanical and energetic behaviors of muscle such as the four phases of a force transient, spontaneous oscillatory contractions, and cardiac pressure–volume loops. From these binding equations, I also re-derive A.V. Hill's muscle equation showing that a binary mechanical model directly accounts for the muscle force–velocity relationship and thus is the "detailed machinery" fit into A.V. Hill's thermodynamic framework.

This model was informed as much by mechanochemical studies of muscle[4] as it was by the principles of thermodynamics, and the thermodynamic lessons learned from muscle provide new insights into systems biology. Muscle is the ideal binary mechanical model system, and

https://doi.org/10.1021/acs.langmuir.2c01622
Langmuir 2022, 38, 15905−15916

much remains to be learned from it about binary mechanical systems in general. Viewed through the lens of thermodynamics instead of rational mechanics, a reanalysis of mechanochemical studies of muscle will provide fundamentally new perspectives on muscle and muscle systems. More broadly, a thermodynamic analysis of muscle provides an unparalleled window into how protein structure−function relationships in general scale up to cellular structure−function relationships under the influence of system energies, macroscopic constraints, entropic forces, and both isothermal and adiabatic reactions.

EXPERIMENTAL SECTION

A binary thermodynamic system consists of N motors (molecular switches) in one of two states (M and AM in Figure 1A). The main assumptions of a binary mechanical model are as follows:

1. A motor, M, undergoes a conformational change induced by track, A, binding (Figure 1A) that moves an unloaded track a distance, d[5,14,18] (the working step).
2. The working step generates a system mechanical potential $F{\cdot}d_{eff}$ when it displaces an effective system spring with stiffness κ_{sys} from an initial displacement, x_{sys}, to a final displacement, $x_{sys} + d_{eff}$, where $F = \kappa_{sys}{\cdot}x_{sys}$ is the force exerted on the spring by the surroundings (Figure 1B).
3. The working step is reversible[18,44,45] (the spring displacement is reversed) with forward, f_+, and reverse, f_-, rate constants defined from first principles. A motor can be irreversibly detached from the track (without reversing the spring displacement) through an active process at a rate ν (Figure 1A).

Molecules, states, and mechanisms known to affect muscle mechanics that are not accounted for in this model (e.g., a small lever arm rotation associated with ADP release[46]) will be incorporated into future models and improve the accuracy with which the model accounts for experimental data.

Binding Free Energy. When the working step occurs against a constant external force, F, the reaction free energy for binding is

$$\Delta_rG = \Delta G^\circ + kT{\cdot}\ln(N_{AM}/N_M) + F{\cdot}d_{eff} \quad (1)$$

where ΔG° is the standard free energy, d_{eff} is an effective motor step size (described below), and N_{AM} and N_M are the number of motors in the AM and M states (the total number of motors is $N = N_{AM} + N_M$). The ligand concentration is constant and implicit in ΔG°. When $\Delta_rG = 0$, eq 1 describes the equilibrium relationship between F and N_{AM}/N_M (the binding isotherm). This relationship is determined energetically, not mechanistically, since along a binding isotherm, the system spring through lengthening or shortening freely exchanges energy with the surroundings.

Thermodynamic Spring. Muscle force, F, in eq 1 can be expressed in terms of a single system spring with stiffness, κ_{sys}, displaced a distance, x_{sys}, or $F = \kappa_{sys}{\cdot}x_{sys}$ (Figure 1B). The work term $F{\cdot}d_{eff}$ in eq 1 is the work performed (i.e., mechanical potential generated) by an M to AM transition in displacing the system spring from a length, x_{sys}, to a length, $x_{sys} + d_{eff}$, or

$$1/2\kappa sys{\cdot}[(x_{sys} + d_{eff})^2 - x_{sys}{}^2] = 1/2\kappa sys{\cdot}d_{eff}{\cdot}[d_{eff} + 2x_{sys}]$$

which when $x_{sys} \gg$; d_{eff} is approximately $\kappa_{sys}{\cdot}x_{sys}{\cdot}d_{eff}$, or $F{\cdot}d_{eff}$.

Adiabatic Force Generation. When muscle is held at a fixed length (the blue barrier in Figure 1B does not move, $x = 0$), the system spring does not exchange energy with the surroundings, and so eq 1 does not apply. Instead, the motor binding reaction collectively generates mechanistically defined forces in the system spring, displacing the spring through increments of d_{eff}. Specifically, both spring displacement, x_{sys}, and force, F, increase with the number of bound motors, $N_{AM} = N - N_M$, as

$$x_{sys} = -d_{eff}(N_M - N_{M^\circ})$$

or

$$F = -\kappa_{sys}{\cdot}d_{eff}(N_M - N_{M^\circ}) \quad (2)$$

where $N_M{}^\circ$ is N_M at $F = 0$. The work performed by a given step ($F{\cdot}d_{eff}$ in eq 1) is obtained by multiplying both sides of eq 2 by d_{eff}, or

$$F{\cdot}d_{eff} = -\kappa_{sys}{\cdot}d_{eff}{}^2(N_M - N_{M^\circ}) \quad (3)$$

Equation 3 is plotted as $F{\cdot}d_{eff}$ versus N_M in Figure 1C (solid black lines with $N_M{}^\circ$ increments of 5).

Binding Isotherm. Collective force generation (eq 2) in the system spring continues until force equilibrates with the binding isotherm at a force, F, defined by eq 1 ($\Delta_rG = 0$):

$$F{\cdot}d_{eff} = -\Delta G^\circ - kT{\cdot}\ln(N_{AM}/N_M) \quad (4)$$

Binding isotherms (eq 4) are plotted as $F{\cdot}d_{eff}$ versus N_M in Figure 1C (colored curves) at ΔG° increments of 1 kT. In Figure 1C, adiabatic force generation occurs along the black line (eq 3, right to left) until force chemically equilibrates with the binding isotherm (eq 4, colored curves).

The time course for force generation is determined by two simple master equations. The first equation is the conventional reaction rate

$$dN_{AM}/dt = -N_{AM}{\cdot}(f_- + \nu) + N_M{\cdot}f_+ \quad (5)$$

The second equation is the rate at which force is generated in the system spring through this reaction, which according to eq 2 is

$$dF/dt = (-N_{AM}{\cdot}f_- + N_M{\cdot}f_+){\cdot}\kappa_{sys}{\cdot}d_{eff} \quad (6)$$

When $\nu = 0$, eqs 5 and 6 describe the kinetics and mechanics of a binding reaction. When $\nu > 0$, an active (ATP-dependent) process irreversibly transfers motors from AM to M without a corresponding change in F (ν does not appear in eq 6), and eqs 5 and 6 describe the kinetics and mechanics of active (ATP-dependent) force generation through a net reaction flux $N_M{\cdot}f_+ > N_{AM}{\cdot}f_-$ (eq 3).

Because the forward, f_+ and reverse, f_-, rate constants are derived from eq 1 (see below), simulations based on eqs 5 and 6 describe adiabatic force generation (eq 3) that implicitly equilibrates along the binding isotherm (eq 4).

Binding Kinetics. At equilibrium, the reaction rate is zero, or $N_{AM}/N_M = f_+/f_-$, which when substituted into eq 4 gives

$$f_+/f_- = \exp[(-F_o{\cdot}d_{eff} - \Delta G^\circ)/kT]$$

For a non-equilibrium reaction, the reaction free energy, δE, pulls the reaction from equilibrium to drive a net binding rate, and

$$f_+/f_- = \exp[(-F_o{\cdot}d_{eff} - \Delta G^\circ - \delta E)/kT] \quad (7)$$

Here, I define δE separate from Δ_rG, to distinguish between the free energy lost from the system as heat and work, Δ_rG, and the effects of Δ_rG on the system, δE (see below). For each energy term, E, in eq 7, the E-dependence of $\exp(E/kT)$ can be partitioned between forward, $f_+(E)$, and reverse, $f_-(E)$, rate constants through a coefficient, a_E, that describes the fractional change in E prior to the activation energy barrier.[47] For example, when δE and F are zero,

$$f_+{}^\circ = \exp(-a_G{\cdot}\Delta G^\circ/kT)$$

and

$$f_-{}^\circ = \exp[(1 - a_G)\,\Delta G^\circ/kT)$$

are the unloaded rate constants.

Chemical and Mechanical Equilibration. If the system spring equilibrates (i.e., freely exchanges energy) with the surroundings, the force of the spring is defined by the external F, and eq 1 applies (F in Figure 1B determines the spring length). If the system spring is held at a fixed length (the blue barrier in Figure 1B does not move) or if force is generated in the system spring faster than the spring equilibrates with the surroundings, changes in F are mechanistically determined by eq 2 (motor displacements in Figure 1B determine the spring length). Equation 2 is a classic adiabatic approximation for

https://doi.org/10.1021/acs.langmuir.2c01622
Langmuir 2022, 38, 15905−15916

force generation in which an idealized system spring does not exchange energy with its surroundings. Force generation deviates from this linear relationship when mechanical equilibration with the surroundings occurs on a time scale comparable to that of force generation.

When active muscle is held at a fixed length, force generation chemically equilibrates ($\Delta_r G = 0$) with an equilibrium binding isotherm that is mechanically equilibrated with a maximal external force, $F = F_o$, from eq 4

$$F = -[\Delta G^\circ + kT\cdot\ln(N_{AM}/N_M)]/d_{eff} \quad (8)$$

Here, the effective displacement, d_{eff}, of a system spring by one of N parallel force generators varies inversely with N, or $d_{eff} = d/N$ because the displacement by one parallel motor is distributed among all other parallel motors. A motor detached from a track is not somehow mechanically isolated from the system (it is still part of the macromolecular assembly) and so d is distributed among all N myosin motors not just the N_{AM} bound motors.[2]

Force generation can chemically equilibrate with forces other than F_o (e.g., a frictional force, an external force held at $F < F_o$, forces in other compliant elements within the system, etc.). For example, when active muscle is held at a fixed force, $F < F_o$, force generation chemically equilibrates with a binding isotherm that is mechanically equilibrated with a sub-maximal force, $a\cdot F_o$, where a is the fraction of the maximal force. In other words, force generation chemically equilibrates with a pseudo-equilibrium binding isotherm, or

$$F = -a\cdot[\Delta G^\circ + kT\cdot\ln(N_{AM}/N_M)]/(d/N)$$

where the non-equilibrium binding free energy $\Delta_r G = (1 - a)\cdot[\Delta G^\circ + kT\cdot\ln(N_{AM}/N_M)]$ is lost from the system as heat and work. Shown below, this is the formal basis for A.V. Hill's force−velocity relationship.[20] In general, d_{eff} in eq 8 equals $d/(a\cdot N)$, where $a = 1$ when the system chemically equilibrates with F_o, and $a < 1$ when the system chemically equilibrates with a pseudo-equilibrated force. Because d_{eff} cannot exceed d, a can never be less than $1/N$.

Force generation can also chemically equilibrate with frictional forces, F_f (see below). If force generation in the system spring is un-damped, a increases linearly and $d_{eff} = d/(a\cdot N)$ decreases inversely with increasing F as described above. According to Huxley−Hill, the distance a motor working step displaces compliant elements external to that motor is $d_{eff} = 0$ (force generation is localized to a motor), which is to say that the working step is fully damped presumably by actin-bound motors that prevent filament sliding.[19,23] According to a chemical thermodynamic model, force generation in a system spring is never fully damped;[19,23] it is maximally damped when force generation chemically equilibrates with a frictional force ($a = 1$) and $d_{eff} = d/N$. In the simulations below, I assume the maximally damped case and will develop the un-damped case separately.

Entropic Force. According to eq 5, when $\Delta G^\circ = 0$, motors can still generate force $F_o = N\cdot kT\ln(N_M/N_{AM})]/d$.

This is an entropic force. Specifically, the entropy of the system is $k\cdot\ln\Omega$, where Ω is the number of available microstates. For a given N_M, there are $\Omega = N!/[N_M!\cdot(N - N_M)!]$ microstates. When one motor binds a ligand, N_M decreases by one, changing the system entropy by

$$\Delta S = k\cdot\ln(N!/[(N_M - 1)!\cdot(N - N_M + 1)!]) - k\cdot\ln(N!/[N_M!\cdot(N - N_M)!])$$

This can be written $\Delta S = -k\cdot\ln[(N_{AM} + 1)/N_M]$, which for large N_{AM} is approximately

$$\Delta S = -k\cdot\ln[N_{AM}/N_M]$$

Thus, $kT\cdot\ln[N_{AM}/N_M]$ in eq 1 is the reaction entropy, $-T\Delta S$, and the force balanced against it is an entropic force.

Computer Simulations. Using master eqs 5 and 6, rate constants defined by eq 7, and model parameters in Table 1, MatLab (Mathworks, Natick, MA) is used to simulate the time course of muscle force transients.

Table 1. Model Parameters.[a]

parameter	description	value
N	number of myosin heads	30 [19]
ΔG°	standard reaction free energy for working step	$-6\ kT$[2]
d	step size	8 nm[13]
κ_{sys}	effective stiffness of system spring	10 pN/nm[59,60]
a_{Go}	partition of standard reaction free energy	0.615[61]
a_{Fd}	partition of work	0.3

[a]The parameter a_{Go} was determined from $f_+^\circ = \exp[a_{Go}\cdot\Delta G^\circ/kT]$ assuming $f_+^\circ = 40\ s^{-1}$ and gives a value for $f_-^\circ = \exp[-(1 - a_{Go})\cdot\Delta G^\circ/kT]$ of $0.1\ s^{-1}$. All other model parameters are determined using first principles (equations derived herein).

RESULTS AND DISCUSSION

Thermodynamic forces are contained within the walls that constrain them (lattices, cylinders, cells, organs, etc.) not within molecules that somehow hold forces within their own walls. There remains no experimental evidence supporting the Huxley−Hill assumption that force generation is localized to a molecular motor. Not even in single molecule mechanics experiments is the force generated by a motor contained within that motor; it is generated in an optical spring external to the motor when that motor displaces an actin filament upon binding.[3] The springs that contain the force generated by a motor exist outside that motor, which in muscle are the springs in the muscle lattice and in all other compliant elements in and around muscle. Motor working steps (Figure 1A) stretch springs in the muscle lattice to generate forces that are thermally equilibrated within the lattice, transferring binding energy (a system chemical potential, Figure 1A) to the lattice in the form of a system mechanical potential energy (Figure 1B). The mechanical potential energy of the lattice can then be transferred back to binding energy upon reversal of the working step. This reversible transfer of system energy is performed not by any one motor but by a change in the distribution of states of a motor ensemble. In other words, chemical thermodynamics as defined by Gibbs applies to muscle; the molecular energetics, kinetics, and mechanics defined by T.L. Hill to formalize Huxley's corpuscular mechanic philosophy does not.

According to eq 4 (colored lines in Figure 1C), F increases with N_M, and according to eq 3 (black lines in Figure 1C), F decreases with N_M. The difference is that eq 4 describes a binding isotherm along which the energy in the spring is freely exchanged with the surroundings and the relationship between F and N_M is defined by energetics independent of mechanism, whereas eq 3 describes an adiabatic binding reaction where the energy in the spring is not exchanged with the surroundings, and the relationship between F and N_M is mechanistically determined.

Complex mechanical behaviors resembling muscle mechanic behaviors emerge from the network of binding pathways in Figure 1C. Adiabatic binding reactions (eq 3, black straight lines in Figure 1C) generate F that approaches a ΔG° isotherm. Isothermal binding reactions (curved colored lines in Figure 1C) occur along the ΔG° isotherm when energy is slowly exchanged with the surrounding as work or heat. Departures from these idealized relationships (lines in Figure 1C) occur when a change in force (a vertical transition in Figure 1C) or a change in chemistry (a vertical transition in Figure 1C for a change in ΔG° or a horizontal transition for

https://doi.org/10.1021/acs.langmuir.2c01622
Langmuir 2022, 38, 15905−15916

irreversible detachments) occurs rapidly relative to binding kinetics. Here, I provide several examples that will be further developed in separate publications. All simulations of time courses are eqs 5 and 6 using parameters from Table 1 unless otherwise specified. I first simulate the mechanical performance of the system when $v = 0$ (i.e., not ATP-driven) before considering active mechanics where $v > 0$ (i.e., ATP-driven).

Thermodynamic Work Loop. Thermodynamic work loops are thermodynamic mechanisms not rational molecular mechanisms. In 1827, Carnot described the work loop for a heat engine[32] as isothermal compression of a gas, adiabatic expansion of a gas, isothermal expansion of a gas, and adiabatic compression of a gas. The equivalent work loop for muscle is isothermal stretch; adiabatic force generation, isothermal shortening, and adiabatic relaxation (Figure 2A).

An isothermal stretch (Figure 2A, pathway 1) occurs along a low affinity ΔG° (= -2 kT) isotherm when the system spring is slowly stretched while remaining equilibrated with the surroundings (eq 4). Two different time courses are simulated in Figure 2B and are replotted as F vs N_M in Figure 2A. Simulations of a slow continuous stretch (Figure 2B, dashed red line) simply follow the isotherm (Figure 2A, dashed red line). Simulations of a small, rapid increase in F through a length step (Figures 2A,B, solid red lines showing jump in force) are followed by simulations of an adiabatic decrease in F (Figures 2A,B, solid red lines returning to isotherm). These simulations are repeated (Figure 2A, red saw tooth steps) to illustrate the mechanism of increased force with stretch along the isotherm.

These simulations (pathway 1) show that force increases with isothermal stretch as $kT{\cdot}\ln(N_{AM}/N_M)/d_{eff}$ (eq 4), which is an entropic contribution to force (see Experimental Section). In other words, isothermal stretch is effectively the elongation of an entropic spring. The sigmoidal shape of the force response to isothermal stretch results from mechanical buffering. That is, over the buffered range ($-1 < \ln[N_M/(N - N_M)] < +1$) force generated by a small lengthening step is partially reversed (buffered) by the decrease in force associated with adiabatic detachment (as illustrated in Figure 2A, red sawtooth). When the entropic spring is stretched beyond the buffered range, the spring becomes increasingly resistant to stretch (the slope, or entropic stiffness, increases) reaching a maximum entropic force of $kT{\cdot}\ln[N - 1]/d_{eff}$ when $N_M = N - 1$. Stretched beyond this force, the one remaining bound motor detaches, and the system spring catastrophically relaxes. Important physiologically, the sigmoidal shape helps to maintain force by requiring increasingly larger forces to detach the last few force-bearing motors.

After an isothermal stretch, force is generated adiabatically (Figure 2A, pathway 2). Following an increase in binding affinity from a ΔG° of -2 kT to -6 kT, simulations of the time course of adiabatic force generation are shown in Figure 2C and replotted as F vs N_M in Figure 2A (pathway 2). These simulations show that F equilibrates with the new binding isotherm, transferring the 4 kT change in binding energy to both mechanical potential in the system spring and a small increase in $kT{\cdot}\ln[N_{AM}/N_M]$. While isothermal stretch is a near-equilibrium process that occurs at an externally defined rate, adiabatic force generation is a non-equilibrium process that occurs at a rate determined by the rate constants in eq 7.

After adiabatic force generation, the system spring shortens isothermally (Figure 2A, pathway 3). This is simply a reversal of an isothermal stretch (pathway 1) only along a higher-energy isotherm. In other words, the entropic spring shortens against a relatively large force, which in a thermodynamic loop is referred to as a power stroke. This thermodynamic power stroke (the shortening of an entropic spring) is not to be confused with the molecular power stroke in Huxley–Hill (the shortening of a molecular spring). Simulations of both discrete (solid red line) and continuous (dashed red line) isothermal shortening are plotted in Figure 2D and replotted as F vs N_M in Figure 2A. Like isothermal stretch, the simulated discrete isothermal shortening steps followed by adiabatic force generation (red sawtooth) show that changes in force during isothermal shortening are buffered.

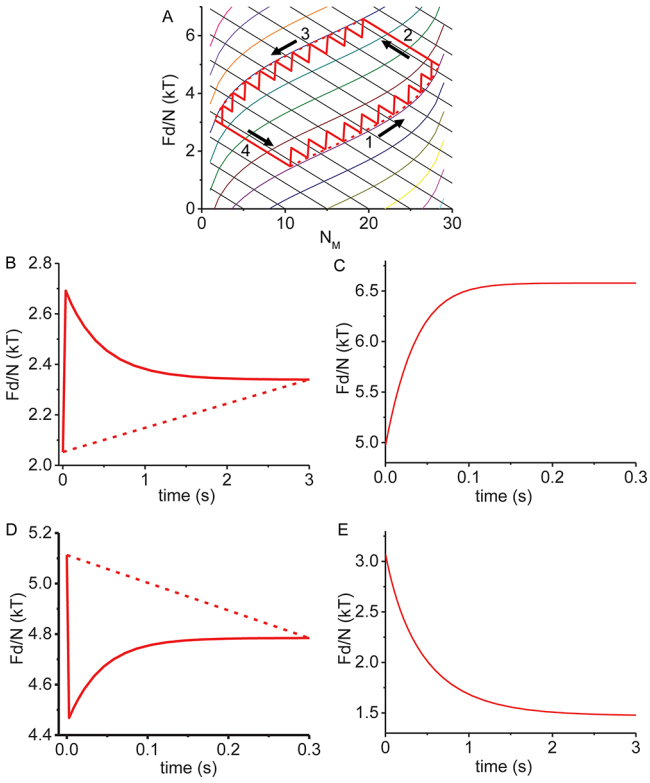

Figure 2. Simulation of a thermodynamic work loop. (A) Four binding pathways of a thermodynamic work loop were simulated (eqs 5 and 6, parameters in Table 1) and plotted against Figure 1C. Isothermal stretch (pathway 1) was simulated both as a slow continuous stretch (dashed red line) and as small discrete stretches that generate force (vertical red lines) and then relax through the reverse adiabatic force generation (red lines parallel to black lines) equilibrating at the $\Delta G^\circ = -2$ kT isotherm. Adiabatic force generation (pathway 2) was simulated following an increase in ΔG° from -2 kT to -6 kT (red line parallel to black lines). Isothermal shortening (pathway 3) was simulated both as a slow continuous shortening (dashed red line) and as small discrete shortening steps (vertical red lines) re-stretched by adiabatic force generation (red lines parallel to black lines) that equilibrates with the $\Delta G^\circ = -6$ kT isotherm. Reversal of adiabatic force generation (pathway 4) was simulated following a decrease in ΔG° from -6 kT to -2 kT (red line parallel to black lines). All simulations in panel (A) were obtained from simulated time courses of force transients using eqs 5 and 6. Examples of time courses for each pathway are in panels (B)–(E). (B) Simulations of isothermal stretch for both discrete steps (one shown, solid line) and continuous stretch (dashed line). (C) Simulations of adiabatic force generation. (D) Simulations of isothermal shortening for both discrete steps (one shown, solid line) and continuous stretch (dashed line). (E) Simulations of the reversal of adiabatic force generation.

https://doi.org/10.1021/acs.langmuir.2c01622
Langmuir 2022, 38, 15905−15916

To complete the thermodynamic cycle, adiabatic force generation is reversed (Figure 2A, pathway 4). Following a decrease in ΔG° from -6 kT to -2 kT, simulations of the time course of the reversal of adiabatic force generation are plotted in Figure 2E and replotted as F vs N_M in Figure 2A (pathway 4). These simulations show that this chemical relaxation transfers the mechanical potential in the system spring to the 4 kT change in binding energy and a small decrease in $kT\cdot\ln[N_{AM}/N_M]$ upon equilibration with the ΔG° (= -2 kT) isotherm.

Like gas expansion in the Carnot cycle, binding can occur with both adiabatic force generation and isothermal shortening (a thermodynamic power stroke). Like gas compression in the Carnot cycle, detachment can occur with both adiabatic force relaxation and isothermal stretch (a thermodynamic recovery stroke). The area inside a thermodynamic loop is the work performed.

This theoretical thermodynamic loop describes reversible binding and detachment reactions in the absence of an active cycle (v = 0), and because it does not involve heat transfer, unlike a Carnot cycle it has a theoretical maximum efficiency of 100%. Practically, however, heat is lost from the system through frictional forces, F_f, (see below) and energy is required to modulate the binding affinity.

Many muscle systems beat periodically, consistent with this thermodynamic work loop. The rapid wing beats of insects and birds occur when antagonistic muscles alternate contractions with the contraction of one muscle stretching the other.[48] The work loop in Figure 2A describes a mechanism by which the thermodynamic power stroke of one muscle can be used to generate the recovery stroke of the other, where the work output can be optimized by changing the binding energy associated with force generation and relaxation (the height of the work loop).

The heart is another muscle system that beats periodically. In fact, the left ventricle of the heart functions through a pressure–volume loop[49] that resembles the mechanics of the thermodynamic loop in Figure 2A. When relaxed, diastolic filling stretches cardiac muscle increasing muscle force along a low-force isotherm (the thermodynamic recovery stroke, Figure 2A, pathway 1). Muscle activation increases the binding energy, and the closure of the mitral valve fixes the length of cardiac muscle so that force is generated adiabatically equilibrating with the high-force isotherm (Figure 2A, pathway 2). Next, the aortic valve opens, allowing cardiac muscle to freely exchange energy with the surroundings while ejecting blood isothermally (the thermodynamic power stroke, Figure 2A, pathway 3). Muscle deactivation decreases the binding energy, and the closure of the aortic valve fixes the length of cardiac muscle so that force is relaxed adiabatically equilibrating with the low-force isotherm (Figure 2A, pathway 4). Through this thermodynamic loop, work performed on the blood by the muscle power stroke along pathway 3 is performed by the blood on the muscle recovery stroke along pathway 1.

We are currently comparing best-fit simulations of this thermodynamic work loop with experimentally obtained pressure-volume loops in the heart. This is the first chemical thermodynamic model of a cardiac work loop and thus has tremendous potential for providing novel biochemical insights into cardiac function in normal and disease states. Indeed, this model implies new physical chemical interpretations for several elements of cardiac pressure-volume loops. For example, the transfer of mechanical potential energy to binding energy through the recovery stroke (Figure 2A, pathway 1) could account for the larger stroke volumes observed by Frank and Starling[50] with increased end diastolic volumes. Specifically, the motors that detach along pathway 1 perform work along pathway 2, and so the further muscle is stretched along pathway 1, the more work is performed along pathway 2.

Force Transients. The different reversible binding pathways in Figure 1C also imply that through a combination of adiabatic and isothermal processes, a single binding reaction can have multiple transient phases following a rapid perturbation. Analogous to the small lengthening and shortening steps simulated in pathways 1 and 3 (Figure 2A), following a rapid increase or decrease in any form of system energy (Figure 3A, phase 1), the system held at a fixed length

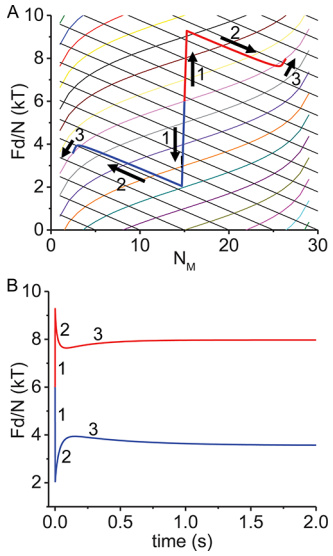

Figure 3. Simulations of force transients. (A) Three phases of a force transient following a rapid increase (phase 1, red) and decrease (phase 1, blue) in force are simulated (eqs 5 and 6, Table 1 parameters) and plotted against Figure 1C. Adiabatic force generation (phase 2, blue) overshoots the ΔG° = -6 kT isotherm by $(1 - a)\Delta G^\circ$ if system forces are not equilibrated at the end of phase 2. Equilibration of forces occurs through isothermal loss (phase 3, blue) or gain (phase 3, red) of $(1 - a)\Delta G^\circ$ as heat to the surroundings at a rate of 4 s^{-1}. (B) Time course of the simulations in panel (A).

responds with adiabatic force generation (eq 3) equilibrating at the ΔG° isotherm (Figure 3A, phase 2). However, unlike in pathways 1 and 3 (Figure 2A), adiabatic force generation need not immediately equilibrate at the ΔG° isotherm. For example, if the distribution of forces (i.e., a) within the system spring equilibrates relatively slowly, adiabatic force generation, F, equilibrates with the $a\cdot\Delta G^\circ$ isotherm (see Experimental Section) before equilibrating with the ΔG° isotherm through an isothermal redistribution of internal forces that mechanically equilibrate at a = 1 (Figure 3A, phase 3). Simulations of the time course of these three phases following both rapid shortening (Figure 3B, blue line) and lengthening (Figure 3B, red line) of the system spring are replotted as F vs N_M in Figure 3A.

Huxley and Simmons observed force transients resembling those in Figure 3B when the length of isometric muscle is rapidly changed.[34] I have compared best-fit simulations to the data in Huxley and Simmons, and the simulated transient

https://doi.org/10.1021/acs.langmuir.2c01622
Langmuir 2022, 38, 15905−15916

amplitudes and rates resemble those reported by Huxley and Simmons (data not shown). I have also compared best-fit simulations to force transients observed by Dantzig et al.[45] following a rapid increase in inorganic phosphate concentrations and have found good agreement with the transient rates and amplitudes that they reported (data not shown).

Active Isometric Force Generation. Work loops and force transients are defined above in the absence of an active cycle (v = 0, Figure 1A). Here, I consider isometric force generation through a relatively slow ATP-dependent active cycle (v > 0). Irreversible detachments (v in Figure 1A) occur through an active process in which AM is transferred to M without a corresponding reversal of force generation. This process requires an energy source (e.g., the free energy for ATP hydrolysis), and through this process the binding equilibrium is perturbed by adding energy,

$\delta E = \Delta_r G(F) = \Delta G^\circ + kT\cdot\ln(N_{AM}/N_M) + F\cdot d_{eff}$ (eq 1), to the system. Because the free energy for ATP hydrolysis is used to increase the binding energy, and the binding energy is then used for work, the energy available for work is the binding energy, $\Delta_r G(F)$, not the free energy for ATP hydrolysis.[3,51] Figure 4 illustrates two of many possible active isometric force-generating trajectories: spontaneous entropic beating (Figure 4A) and force recovery (Figure 4B). The ATP-dependent irreversible detachment of motors is shown in Figure 4A as an increase in N_M without a change in F (horizontal red line segments).

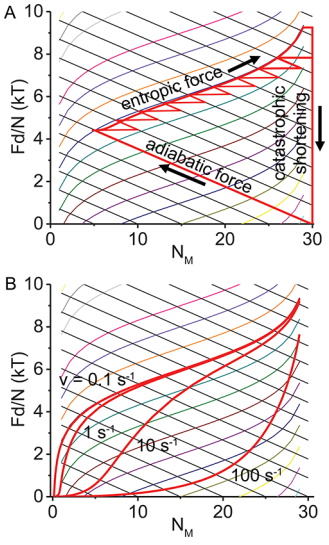

Figure 4. Simulations of active (v > 0) isometric force generation. (A) Entropic beating starts with F = 0 and N_M = 30. Simulated adiabatic force generation (red line) occurs rapidly along an adiabatic binding curve (black lines) equilibrating with the ΔG° = −6 kT isotherm. Entropic force generation then occurs through the reaction cycle (v). Both discrete and continuous simulations of entropic force generation are simulated. Continuous simulations are performed using eqs 5 and 6 with a rate, v, of 1 s^{-1}. Discrete simulations are irreversibly detachment (ΔN_M = 5, horizontal red line segments) followed by simulations of adiabatic force generation that equilibrates with the ΔG° = −6 kT. Entropic force generation continues until no motors are bound, at which point the system spring catastrophically shortens returning to initial conditions (F = 0, N_M = 30). (B) Force recovery starts with F = 0 and N_M = 0. Force generation occurs through the reaction cycle like entropic force generation in panel (A).

Spontaneous beating (Figure 4A) begins in a non-equilibrium state with $N_M = N$ (no motors bound), F = 0, and ΔG° = −6 kT. Equivalent to pathway 2 in a thermodynamic loop (Figure 2A) and phase 2 in a force transient (Figure 3), simulated adiabatic force generation (Figure 4A, solid red line) occurs along an adiabatic binding curve (eq 3) and rapidly (faster than v) equilibrates with the ΔG° isotherm. Force generation then continues at a slower rate through irreversible detachments, v, following a mechanism that resembles an isothermal stretch (Figure 2A, pathway 1); only here, the steps that perturb the system from equilibrium are chemical (v) not mechanical. The difference is that mechanical steps in an isothermal stretch are vertical transitions away from the isotherm (Figure 1C), whereas irreversible chemical steps are horizontal transitions away from the isotherm (increments of ΔN_M = 5 with no change in F; Figure 4A, horizontal red line segments). Like a mechanical perturbation, simulations following a chemical perturbation show that force generation (red lines parallel to eq 3) re-equilibrates with the ΔG° isotherm. The smooth red "entropic force" line in Figure 4A is a simulation of a slow continuous reaction, v. Like with an isothermal stretch, active force generation along the isotherm continues until the entropic force equals $kT\cdot\ln[N - 1]/d_{eff}$ when $N_M = N - 1$, beyond which the last motor detaches and the system spring catastrophically relaxes (Figure 4A) returning the system to its initial state ($N_M = N$, F = 0, and ΔG° = −6 kT).

This entropic cycle repeats leading to periodic force generation, consistent with spontaneous oscillatory contractions observed under certain conditions in muscle and other actin−myosin systems.[52−55] Unlike the counterclockwise thermodynamic work loop (Figure 2A), however, the area inside the clockwise entropic force loop is energy lost from the system as heat, not work, illustrating why entropy cannot be used for work performed on the surroundings. We are currently comparing best-fit simulations to spontaneous oscillations experimentally observed in different systems, including the periodic beating generated by small ensembles of myosin motors observed in vitro. We have developed thermodynamic Monte Carlo models to simulate the discrete force-generating steps observed in some of these studies.[52]

Steady-state (constant, not beating) forces observed in most muscle and actin−myosin systems require that entropic force in the system spring is lost from the system through a continuous isothermal process (similar to phase 3 in a force transient, Figure 3) and not through the catastrophic heat loss of entropic beating. In this case, a steady-state force is reached when $N_M = N_{AM}$, consistent with the observed distribution of states in isometric muscle.[22]

A distinctly different force generating pathway (Figure 4B) begins in a non-equilibrium state where N_M = *0* (all motors are bound), F = 0, and ΔG° = −6 kT. Fast adiabatic force generation cannot occur from this state because no adiabatic binding pathways (eq 3) lead out of it. Here, force generation occurs through the reaction cycle at a rate, v, (Figure 4B, slow kinetics) first equilibrating with the ΔG° isotherm before generating force along it. Simulations of continuous force generation are plotted as F vs N_M in Figure 4B at values for v of 0.1, 1, 10, and 100 s^{-1}, showing that when v increases relative to binding kinetics, the reaction is pulled from equilibrium and falls short of the ΔG° isotherm, limiting force generation. We are currently comparing best-fit simulations to force redevelopment[56] observed in muscle fibers through a protocol of a large

https://doi.org/10.1021/acs.langmuir.2c01622
Langmuir 2022, 38, 15905−15916

shortening step of isometric muscle followed by a rapid re-stretch. The simulations in Figure 4B are consistent with force redevelopment if rapid binding and a redistribution of forces immediately follows the large shortening step.

Steady-State Isotonic Shortening. As described above, in an isometric system, adiabatic force generation equilibrates with the ΔG° isotherm when $F_o = N{\cdot}\Delta G^\circ/d$ (eq 8, $a = 1$, $N_{AM} = N_M$). In an isotonic system, the system is held at a constant force, $F < F_o$, and force generation reaches an pseudo $a{\cdot}\Delta G^\circ$ isotherm when $F = a{\cdot}N{\cdot}\Delta G^\circ/d$ (eq 8).

When muscle shortens against a constant force, F, it is constrained neither by adiabatic force generation (fixed length) nor the binding isotherm (equilibrium), and so the binding pathways in Figure 1C, while still informative, are not strictly followed. Nevertheless, it is instructive to first consider simulations of steady-state isometric shortening occurring through sequential mechanisms of adiabatic force generation followed by an isothermal power stroke. Figure 5 shows

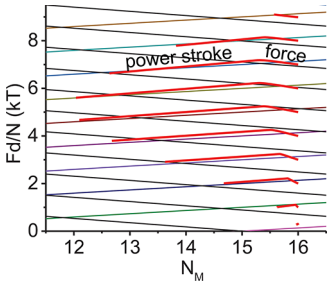

Figure 5. Simulations of single isotonic reaction cycles at different forces, F. Starting from $N_M = 15$ and F set to a value that satisfies equilibrium conditions (eq 1, $\Delta_rG = 0$), one motor is irreversibly transferred from AM to M, increasing N_M to 16 and adding energy, $\delta E = \Delta_rG = \Delta G^\circ + F{\cdot}d_{eff}$ to the system (horizontal line not shown). Simulated (eqs 5 and 6, Table 1 parameters) adiabatic force generation equilibrates with the $a{\cdot}\Delta G^\circ$ isotherm. Loss of Δ_rG from the system by shortening of the system spring (power stroke) is simulated at a rate of 0.8 s^{-1}.

simulations of individual steady-state reaction cycles at different forces, F. Starting at equilibrium conditions with $N_M = 15$, irreversible detachment of one motor through v perturbs the system from equilibrium adding energy, $\delta E = \Delta G^\circ + F{\cdot}d_{eff}$, to the system. This corresponds to a horizontal transition in Figure 5 from $N_M = 15$ to $N_M = 16$ (not shown). The simulated response is adiabatic force generation (Figure 5, red line labeled "force") followed by an isothermal power stroke (Figure 5, red line labeled "power stroke"). Figure 5 shows that when the system is held at a maximum force, $F_o = \Delta G^\circ/d_{eff}$, entropic force F is generated with no subsequent power stroke since no energy is available for work. As described above, this entropic force must be lost as heat to complete a steady-state cycle (i.e., return to $N_M = 15$). Figure 5 shows that when the system is held at intermediate forces, F, the energy available for work exceeds by nearly four-fold ($\Delta N_M > 1$) the work that can be performed by the power stroke of a single motor ($\Delta N_M = 1$). At low F, a becomes small, and the relatively large amount of work required by motors to equilibrate with the $a{\cdot}\Delta G^\circ$ isotherm begins to stall force-generating kinetics ($\Delta N_M < 1$). The minimum F is that generated by one motor ($a = 1/N$), and at this force (Figure 5, red dot) neither force generation nor a power stroke occur.

Figure 5 illustrates the significant inefficiencies associated with formally separating adiabatic force generation from the isothermal power stroke. At intermediate forces, the energy available for work exceeds by nearly four-fold the work that can be performed with a single step (from $N_M = 16$ to 15). At low forces, the work required for adiabatic force generation stalls the reaction, which is a fundamental flaw with the Huxley–Hill power stroke mechanism. While Huxley–Hill requires that molecular force generation and the power stroke are formally separated, in a thermodynamic model of muscle shortening against a constant force, F, there are no fixed length (adiabatic) or equilibrium (isothermal) constraints, which is to say that the binding reaction is constrained by neither eq 3 nor 4 (the lines in Figure 5). There is only the constraint of a constant force, F.

Unlike the simulations in Figure 5, if we constrain the reaction with a constant force, F, and $\Delta N_{AM} = 1$, the distance shortened, x, against that force is $x = \Delta_rG/F$. The maximum isometric force, $F_o = N{\cdot}\Delta G^\circ/d$ (assuming $N_{AM} = N_M$) can be substituted into eq 1 to obtain the energy available for work by a working step

$$\Delta_rG = (F_o{\cdot}d - F{\cdot}d)/N$$

Expanding upon our previous analysis,[2] the distance moved by N motors is

$$x = \Delta_rG/F = (F_o - F){\cdot}d/F$$

If we take into consideration movement, x against frictional (dissipative) forces, F_f ,

$$x = \Delta_rG/F = (F_o - F){\cdot}d/(F + F_f)$$

the rate of movement (the velocity, $V = dx/dt$) is

$$V = v{\cdot}(F_o - F){\cdot}d/(F + F_f)$$

where v is the ATP-dependent rate of the reaction cycle. This equation can be rewritten

$$v{\cdot}(F_o - F){\cdot}d = F{\cdot}V + F_f{\cdot}V \quad (9)$$

which is essentially the binary mechanical model fitted into A.V. Hill's formalism. Indeed, to characterize the relationship between muscle force, F, and muscle shortening velocities, V, muscle physiologists universally use Hill's $F–V$ equation:

$$b_H(F_o - F) = F{\cdot}V + a_H{\cdot}V$$

This equation is widely considered to be phenomenological when, in fact, it is based on first principles (eq 9) with $b_H = v{\cdot}d$ and $a_H = F_f$.

For most muscle types, A.V. Hill's muscle equation (i.e., eq 9) accurately fits experimentally obtained muscle force-velocity relationships. Because eq 9 was derived directly from a binary thermodynamic model, this model accurately accounts for observed muscle force-velocity relationships in muscle. The term F_fV in eq 9 describes the rate at which work is performed against a frictional load, F_f, which is the rate at which heat is lost with shortening muscle. This term corresponds to the term $a_H{\cdot}V$ in Hill's model, which he described as the shortening heat. Equation 7 predicts that the heat of shortening increases linearly with V, roughly consistent with Hill's observations.[20] Observed non-linearities in this relationship[4] could be accounted for in this model by an F-dependent frictional load, F_f.

https://doi.org/10.1021/acs.langmuir.2c01622
Langmuir 2022, 38, 15905–15916

Unloaded Shortening, *Vo*. According to eq 9, when $F = 0$, the maximum unloaded shortening velocity is energetically defined as

$$V_o = F_o \cdot v \cdot d / F_f$$

For comparison, the kinetic definition of V_o is simply the product of the stepping rate, $N \cdot v$, and the apparent step size, d_{eff}, or

$$V_o = N \cdot v \cdot d_{eff} = v \cdot d / a$$

Combined, the energetic and kinetic definitions of V_o give

$$a = F_f / F_o$$

which when written as $a \cdot F_o = F_f$, is simply a chemical expression of Newton's third law (the chemical force generated by motors is balanced by the frictional force against which they shorten). As described above, the minimum value for $a = F_f/F_o$ is $1/N$. Assuming F_f is imposed by resistive motors, F_f/F_o decreases with increasing N until the effects of N on F_f and F_o are proportional at which point this saturating N sets a lower limit for a of $a_{min} = 1/N$.

There are two limits to V_o. A minimum V_o $(= v \cdot d)$ is energetically limited by $F_f = F_o$ (F_f cannot exceed the maximum force generated, F_o), which is to say that adiabatic force generation equilibrates with F_f $(a = 1)$. This is the rate of force generation assumed in the analyses above. A maximum V_o $(= v \cdot d / a_{min})$ is kinetically limited at $a = a_{min}$.

In muscle, V_o exceeds $v \cdot d$ by a factor of approximately 5 to 10,[57,58] which according to the above analysis implies a_{min} values of 0.1 to 0.2. Using an in vitro motility assay, we have demonstrated that V_o is not energetically limited $(a < 1)$[18,19,23,24,42] and have recently estimated a value for $a = F_f/F_o$ in this assay of approximately 0.4.[19] Values for $a_{min} = a_H/F_o$ obtained from measurements of muscle F-V relationships typically range from 0.2 to 0.3.[4]

Epilogue. Assigning familiar mechanical devices and structures ("rational mechanics") to particles that exist on a scale that we cannot comprehend is common throughout scientific history and is a practice that continues today in some scientific communities. The extent to which this "rational" mechanical thought fails us is best understood through historical accounts. The mechanistic difference between Boyle's "springs of air" and the kinetic theory of gas is profound and represents a radical advance in scientific thought brought about by thermodynamics. This same radical advance in scientific thinking underlies the profound difference between "rational" molecular mechanisms of physiological function and thermodynamic mechanisms of physiological function. We must understand this difference before thermodynamics can transform molecular biology; that, or we remain tethered to a 17th century worldview of molecular cartoons.

Single molecule kinetic, structural and mechanic studies show that binding of a myosin motor to an actin filament induces a switch-like lever arm rotation that displaces an actin filament. From this molecular mechanism, we will never find a rational mechanism of muscle contraction because we lack the "fineness of perception" to reason a connection. However, from this molecular mechanism we can determine thermodynamic mechanisms of muscle contraction. While it may seem odd from a 17th century rational mechanics perspective, the physiological function of this molecular mechanism cannot be determined from the mechanism itself; it must also be determined from external constraints on muscle. As I have shown, when muscle is free to shorten, this mechanism performs work. When muscle is held at a fixed length, this mechanism generates force. When muscle is allowed to contract against a constant force, this mechanism both generates force and performs work. Based on a single molecular mechanism, these are the thermodynamic mechanisms of muscle contraction.

It has taken over 80 years to fit the "detailed machinery" into A.V. Hill's thermodynamic model of muscle contraction. Key to this development was constructing a system spring. This entropic spring resembles other well-known entropic springs that contain molecular switches such as titin[41] and rubber[43] with several significant differences. First, muscle is not a polymer since the switch linkages between actin and myosin filaments reversibly detach. The length of the entropic spring is chemically defined by N_M/N_{AM} with a maximum length that is reached when $N_M/N_{AM} = (N - 1)$. While longer than a molecular spring, the entropic spring is still relatively short. Unlike other entropic springs, in muscle the switches are not passive; rather, they catalyze the hydrolysis of ATP and irreversibly change states through this active process. The irreversible increase in binding energy through the catalyzed reaction (an increase N_M/N_{AM} in eq 1) in effect adds energy to the entropic spring chemically lengthening it. The relaxation of the binding reaction (a decrease in N_M/N_{AM} in eq 1) is in effect the shortening of the entropic spring (a thermodynamic power stroke). The molecular power stroke model attributes to a molecule this macroscopic power stroke mechanism, which accounts for its moderate success at modeling certain aspects of muscle contraction. However, while a molecular spring is a familiar rational device that we can use to imagine a thermodynamic force contained within a corpuscle, there are no comparable molecular vessels for containing concentration gradients, system entropy, and adiabatic and isothermal processes (e.g., work loops).

Thermodynamics has transformed our understanding of how systems of molecules work, yet its transformative power has yet to reach many areas of molecular biology. Rational mechanisms that depict physiological function in terms of molecular cartoons are grossly inventive and non-physical, often differing dramatically from the actual thermodynamic mechanisms. A thermodynamic model of muscle contraction describes muscle mechanics in terms of protein structural states, system mechanics, system energetics, and kinetics. Structural and mechanical details of muscle proteins provide useful insights into their average effects on thermodynamic parameters but can mislead when used to characterize rational building blocks.

AUTHOR INFORMATION

Corresponding Author

Josh E. Baker − *Department of Pharmacology, University of Nevada, School of Medicine, Reno, Nevada 89557, United States;* orcid.org/0000-0002-2101-5215; Email: jebaker@unr.edu

Complete contact information is available at: https://pubs.acs.org/10.1021/acs.langmuir.2c01622

Notes

The author declares no competing financial interest.

https://doi.org/10.1021/acs.langmuir.2c01622
Langmuir 2022, 38, 15905−15916

■ ACKNOWLEDGMENTS

I thank JWG, AVH, Julie, my students, colleagues, and mentors who have over many years inspired and guided this work. This work was funded by a grant from the National Institutes of Health 1R01HL090938-01.

■ REFERENCES

(1) Kittel, C.; Kroemer, H.*Thermal Physics*; 1980.
(2) Baker, J. E.; Thomas, D. D. A Thermodynamic Muscle Model and a Chemical Basis for A.V. Hill's Muscle Equation. *J. Muscle Res. Cell Motil.* **2000**, *21*, 335−344.
(3) Baker, J. E. A Chemical Thermodynamic Model of Motor Enzymes Unifies Chemical-Fx and Powerstroke Models. *Biophys. J.* **2022**, *121*, 1184−1193.
(4) Woledge, R. C.; Curtin, N. A.; Homsher, E.*Energetic Aspects of Muscle Contraction*, 41st ed.; Monogr. Physiol. Society, 1985.
(5) Finer, J. T.; Simmons, R. M.; Spudich, J. A. Single Myosin Molecule Mechanics: Piconewton Forces and Nanometre Steps. *Nature* **1994**, *368*, 113−119.
(6) Huxley, H. E. The Mechanism of Muscular Contraction. *Science* **1969**, *164*, 1356−1366.
(7) Sabido-David, C.; Hopkins, S. C.; Saraswat, L. D.; Lowey, S.; Goldman, Y. E.; Irving, M. Orientation Changes of Fluorescent Probes at Five Sites on the Myosin Regulatory Light Chain during Contraction of Single Skeletal Muscle Fibres. *J. Mol. Biol.* **1998**, *279*, 387−402.
(8) Baker, J. E.; Brust-Mascher, I.; Ramachandran, S.; LaConte, L. E.; Thomas, D. D. A Large and Distinct Rotation of the Myosin Light Chain Domain Occurs upon Muscle Contraction. *Proc. Natl. Acad. Sci. U. S. A.* **1998**, *95*, 2944−2949.
(9) Huxley, A. F. Muscular Contraction. *J. Physiol.* **1974**, *243*, 1−43.
(10) Rayment, I.; Rypniewski, W. R.; Schmidt-Bäse, K.; Smith, R.; Tomchick, D. R.; Benning, M. M.; Winkelmann, D. A.; Wesenberg, G.; Holden, H. M. Three-Dimensional Structure of Myosin Subfragment-1: A Molecular Motor. *Science* **1993**, *261*, 50−58.
(11) Uyeda, T. Q.; Abramson, P. D.; Spudich, J. A. The Neck Region of the Myosin Motor Domain Acts as a Lever Arm to Generate Movement. *Proc. Natl. Acad. Sci. U. S. A.* **1996**, *93*, 4459−4464.
(12) Llinas, P.; Pylypenko, O.; Isabet, T.; Mukherjea, M.; Sweeney, H. L.; Houdusse, A. M. How Myosin Motors Power Cellular Functions: An Exciting Journey from Structure to Function. *FEBS J.* **2013**, *279*, 551−562.
(13) Guilford, W. H.; Dupuis, D. E.; Kennedy, G.; Wu, J.; Patlak, J. B.; Warshaw, D. M. Smooth Muscle and Skeletal Muscle Myosins Produce Similar Unitary Forces and Displacements in the Laser Trap. *Biophys. J.* **1997**, *72*, 1006−1021.
(14) Molloy, J. E.; Burns, J. E.; Sparrow, J. C.; Tregear, R. T.; Kendrick-Jones, J.; White, D. C. Single-Molecule Mechanics of Heavy Meromyosin and S1 Interacting with Rabbit or Drosophila Actins Using Optical Tweezers. *Biophys. J.* **1995**, *68*, 298S−303S.
(15) Lymn, R. W.; Taylor, E. W. Mechanism of Adenosine Triphosphate Hydrolysis by Actomyosin. *Biochemistry* **1971**, *10*, 4617−4624.
(16) Goldman, Y. E. Kinetics of the Actomyosin ATPase in Muscle Fibers. *Annu. Rev. Physiol.* **1987**, *49*, 637−654.
(17) Cooke, R. Actomyosin Interaction in Striated Muscle. *Physiol. Rev.* **1997**, *77*, 671−697.
(18) Baker, J. E.; Brosseau, C.; Joel, P. B.; Warshaw, D. M. The Biochemical Kinetics Underlying Actin Movement Generated by One and Many Skeletal Muscle Myosin Molecules. *Biophys. J.* **2002**, *82*, 2134−2147.
(19) Stewart, T. J.; Murthy, V.; Dugan, S. P.; Baker, J. E. Velocity of Myosin-Based Actin Sliding Depends on Attachment and Detachment Kinetics and Reaches a Maximum When Myosin Binding Sites on Actin Saturate. *J. Biol. Chem.* **2021**, No. 101178.
(20) Hill, A. V. The Heat of Shortening and the Dynamic Constants of Muscle. *Proc. R. Soc. London. Ser. B* **1938**, *126*, 136−195.
(21) Hill, A. V. The Effect of Load on the Heat of Shortening of Muscle. *Proc. R. Soc. London. Ser. B* **1964**, *159*, 297−318.
(22) Baker, J. E.; LaConte, L. E. W.; Brust-Mascher, I.; Thomas, D. D. Mechanochemical Coupling in Spin-Labeled, Active, Isometric Muscle. *Biophys. J.* **1999**, *77*, 2657−2664.
(23) Hooft, A. M.; Maki, E. J.; Cox, K. K.; Baker, J. E. An Accelerated State of Myosin-Based Actin Motility. *Biochemistry* **2007**, *46*, 3513−3520.
(24) Stewart, T. J.; Jackson, D. R.; Smith, R. D.; Shannon, S. F.; Cremo, C. R.; Baker, J. E. Actin Sliding Velocities Are Influenced by the Driving Forces of Actin-Myosin Binding. *Cell. Mol. Bioeng.* **2013**, *6*, 26−37.
(25) Hill, A. V.*Trails and Trials in Physiology: A Bibliography, 1909−1964; with Reviews of Certain Topics and Methods and a Reconnaissance for Further Research*; Williams and Wilkins: Baltimore, MD, 1966.
(26) Huxley, H.; Hanson, J. Changes in the Cross-Striations of Muscle during Contraction and Stretch and Their Structural Interpretation. *Nature* **1954**, *173*, 973−976.
(27) Huxley, A. F.; Niedergerke, R. Structural Changes in Muscle during Contraction. *Nature* **1954**, *173*, 971−973.
(28) Hill, T. L. Theoretical Formalism for the Sliding Filament Model of Contraction of Striated Muscle. Part I. *Prog. Biophys. Mol. Biol.* **1974**, *28*, 267−340.
(29) Huxley, A. F. Muscle Structure and Theories of Contraction. *Prog. Biophys. Biophys. Chem.* **1957**, *7*, 255−318.
(30) Boyle, R.*A Defence of the Doctrine Touching the Spring and Weight of the Air*; London: Printed by F.G. for Thomas Robinson, 1662.
(31) Amontons, G.*Method of Substituting the Force of Fire for Horse and Man Power to Move Machines*. Philos. Hist. Mem. R. Acad. Sci. Paris. Transl. by Martyn Chambers.London1742.
(32) Carnot, S.*Reflections on the Motive Power of Fire*; Dover, 2005.
(33) Månsson, A. Hypothesis: Single Actomyosin Properties Account for Ensemble Behavior in Active Muscle Shortening and Isometric Contraction. *Int. J. Mol. Sci.* **2020**, *21*, 1−21.
(34) Huxley, A. F.; Simmons, R. M. Proposed Mechanism of Force Generation in Striated Muscle. *Nature* **1971**, *233*, 533−538.
(35) Campbell, K. S. Filament Compliance Effects Can Explain Tension Overshoots during Force Development. *Biophys. J.* **2006**, *91*, 4102−4109.
(36) Chase, P. B.; Macpherson, J. M.; Daniel, T. L. A Spatially Explicit Nanomechanical Model of the Half-Sarcomere: Myofilament Compliance Affects Ca 2+-Activation. *Ann. Biomed. Eng.* **2004**, *32*, 1559−1568.
(37) Jarvis, K. J.; Bell, K. M.; Loya, A. K.; Swank, D. M.; Walcott, S. Force-Velocity and Tension Transient Measurements from Drosophila Jump Muscle Reveal the Necessity of Both Weakly-Bound Cross-Bridges and Series Elasticity in Models of Muscle Contraction. *Arch. Biochem. Biophys.* **2021**, *701*, No. 108809.
(38) Pertici, I.; Bongini, L.; Melli, L.; Bianchi, G.; Salvi, L.; Falorsi, G.; Squarci, C.; Bozó, T.; Cojoc, D.; Kellermayer, M. S. Z.; Lombardi, V.; Bianco, P. A Myosin II Nanomachine Mimicking the Striated Muscle. *Nat. Commun.* **2018**, *9*, 3532.
(39) Campbell, K. Rate Constant of Muscle Force Redevelopment Reflects Cooperative Activation as Well as Cross-Bridge Kinetics. *Biophys. J.* **1997**, *72*, 254−262.
(40) Gibbs, J.*Elementary Principles in Statistical Mechanics Developed with Especial Reference to the Rational Foundation of Thermodynamics*; 1902.
(41) Kellermayer, M. S.; Smith, S. B.; Granzier, H. L.; Bustamante, C. Folding-Unfolding Transitions in Single Titin Molecules Characterized with Laser Tweezers. *Science* **1997**, *276*, 1112−1116.
(42) Brizendine, R. K.; Sheehy, G. G.; Alcala, D. B.; Novenschi, S. I.; Baker, J. E.; Cremo, C. R. A Mixed-Kinetic Model Describes Unloaded Velocities of Smooth, Skeletal, and Cardiac Muscle Myosin Filaments in Vitro. *Sci. Adv.* **2017**, *3*, No. eaao2267.
(43) Phys, J. C.; Hanson, D. E. The Molecular Kink Paradigm for Rubber Elasticity : Numerical Simulations of Explicit Polyisoprene Networks at Low to Moderate Tensile Strains of Explicit Polyisoprene

Networks at Low to Moderate Tensile Strains. *J. Chem. Phys.* **2011**, *135*, No. 054902.
(44) Pate, E.; Cooke, R. A Model of Crossbridge Action: The Effects of ATP, ADP and Pi. *J. Muscle Res. Cell Motil.* **1989**, *10*, 181−196.
(45) Dantzig, J.; Goldman, Y.; Millar, N.; Lacktis, J.; Homsher, E. Reversal of the Cross-Bridge Force-Generating Transition by Photogeneration of Phosphate in Rabbit Psoas Muscle Fibres. *J. Physiol.* **1992**, *451*, 247.
(46) Veigel, C.; Molloy, J. E.; Schmitz, S.; Kendrick-jones, J. Load-Dependent Kinetics of Force Production by Smooth Muscle Myosin Measured with Optical Tweezers. *Nat. Cell Biol.* **2003**, *5*, 980−986.
(47) Hille, B.*Ionic Channels of Excitable Membranes*2nd Edition. Sinauer associates: Sunderland, MA, 1987.
(48) Iwamoto, H.; Yagi, N. The Molecular Trigger for High-Speed Wing Beats in a Bee. *Science* **2013**, *341*, 1243−1247.
(49) Suga, H. Cardiac Energetics : From Emax to Pressure-Volume Area. *Clin. Exp. Pharmacol. Physiol.* **2003**, *30*, 580−585.
(50) Sequeira, V.; Van Der Velden, J. Historical Perspective on Heart Function : The Frank − Starling Law. *Biophys Rev* **2015**, *7*, 421−447.
(51) Baker, J. E. Free Energy Transduction in a Chemical Motor Model. *J. Theor. Biol.* **2004**, *228*, 467−476.
(52) Hwang, Y.; Washio, T.; Hisada, T.; Higuchi, H.; Kaya, M. A Reverse Stroke Characterizes the Force Generation of Cardiac Myofilaments, Leading to an Understanding of Heart Function. *Proc. Natl. Acad. Sci. U. S. A.* **2021**, *118*, 1−11.
(53) Fabiato, A.; Fabiato, F. Myofilament-Generated Tension Oscillations during Partial Calcium Activation and Activation Dependence of the Sarcomere Length-Tension Relation of Skinned Cardiac Cells. *J. Gen. Physiol.* **1978**, *72*, 667−699.
(54) Martin, P.; Bozovic, D.; Choe, Y.; Hudspeth, A. J. Spontaneous Oscillation by Hair Bundles of the Bullfrog's Sacculus. *J. Neurosci.* **2003**, *23*, 4533−4548.
(55) Pecreaux, J.; Röper, J. C.; Kruse, K.; Jülicher, F.; Hyman, A. A.; Grill, S. W.; Howard, J. Spindle Oscillations during Asymmetric Cell Division Require a Threshold Number of Active Cortical Force Generators. *Curr. Biol.* **2006**, *16*, 2111−2122.
(56) Brenner, B. Effect of Ca2+ on Cross-Bridge Turnover Kinetics in Skinned Single Rabbit Psoas Fibers: Implications for Regulation of Muscle Contraction. *Proc. Natl. Acad. Sci. U. S. A.* **1988**, *85*, 3265−3269.
(57) Tyska, M. J.; Warshaw, D. M. The Myosin Power Stroke. *Cell Motil. Cytoskeleton* **2002**, *15*, 1−15.
(58) Howard, J.*Mechanics of Motor Proteins and the Cytoskeleton*, 1st ed.; Sinauer Associates, 2001.
(59) Ford, L. E.; Huxley, A. F.; Simmons, R. M. The Relation between Stiffness and Filament Overlap in Stimulated Frog Muscle Fibres. *J. Physiol.* **1981**, *311*, 219−249.
(60) Lewalle, A.; Steffen, W.; Stevenson, O.; Ouyang, Z.; Sleep, J. Single-Molecule Measurement of the Stiffness of the Rigor Myosin Head. *Biophys. J.* **2008**, *94*, 2160−2169.
(61) Pertici, I.; Bianchi, G.; Bongini, L.; Cojoc, D.; Taft, M. H.; Manstein, D. J.; Lombardi, V.; Bianco, P. Muscle Myosin Performance Measured with a Synthetic Nanomachine Reveals a Class-Specific Ca2+-Sensitivity of the Frog Myosin II Isoform. *J. Physiol.* **2021**, *599*, 1815−1831.

https://doi.org/10.1021/acs.langmuir.2c01622
Langmuir 2022, 38, 15905−15916